

1     **New evidence for a major late-Quaternary submarine landslide on the**  
2                                   **external western levee of Laurentian Fan**

3     Alexandre Normandeau, D. Calvin Campbell, David J.W. Piper, Kimberley A. Jenner  
4     *Geological Survey of Canada (Atlantic), Natural Resources Canada, 1 Challenger Drive,*  
5                                   *Dartmouth, Nova Scotia, Canada, B2Y 4A2*

6  
7     **Abstract:** The Laurentian Fan is one of the largest submarine fans on the western margin  
8     of the North Atlantic. Recently acquired high-resolution multibeam bathymetric data (60  
9     m horizontal resolution) reveal a major mass transport deposit (MTD) on the Western  
10    Levee of Western Valley (WLWV), covering >14 000 km<sup>2</sup> in water depths from 3900 m  
11    to >5000 m. Typical submarine landslide features are observed such as headscarps that in  
12    places reach the crest of the levee, crown cracks, extensional ridges, blocky debris and flow  
13    lineations. Multiple headwalls are observed on 3.5 kHz sub-bottom profiles indicating that  
14    the landslide retrogressed upslope. While the upper parts of the MTD consist of intact  
15    blocks that were displaced downslope as ridges and troughs, the lower parts exhibit a ~30  
16    m thick incoherent to transparent acoustic facies typical of debris flows. Landslide  
17    geomorphology thus suggests that it was generated as a retrogressive spread and that slide  
18    blocks disintegrated downslope to become a blocky landslide with a surficial debris flow.  
19    The blocky landslide/debris flow extends downslope ~90 km and partially fills a submarine  
20    channel. The superposition of the MTD filling the channel and its location at the top of the  
21    stratigraphic succession in the levee suggests that it is late Quaternary in age, possibly  
22    Holocene. Deeper seismic reflection data also show that this is a rare event during the  
23    Quaternary; it is the largest MTD observed in the upper ~375 m of the levee succession  
24    and among the largest and deepest in the Western North Atlantic.

25    **Introduction**

26    Submarine landslides play an important role in the evolution of active and passive margins  
27    by transporting large volumes of sediment to the deep-sea. They commonly occur on steep  
28    slopes, where sedimentary deposits are thick (Hampton et al. 1996). Submarine canyon

29 environments are prime locations for the generation of landslides because they supply large  
30 volumes of sediment and are characterized by steep slopes (e.g., Jenner et al., 2007).  
31 Typically, landslides tend to be small and relatively frequent along canyon or channel  
32 margins (e.g., Smith et al., 2005) whereas they are typically much larger and infrequent in  
33 inter-canyon (or open) slopes (Lee, 2009).

34 Offshore Nova Scotia, large and infrequent submarine landslides have been reported on the  
35 Scotian margin through the analysis of multibeam bathymetry and seismic stratigraphy  
36 (e.g., Piper et al., 2003; Mosher et al., 2004). Landslide scars are widespread both on the  
37 open slopes and on the inner canyon environments. The Laurentian Fan valleys, extending  
38 from the Laurentian Channel, are no exception to the presence of submarine landslides. As  
39 an example, they were the main conduits for the 1929 Grand Banks failure (Piper and Aksu,  
40 1987; Piper et al., 1999). Because the fan valleys were fed by glacial sediments  
41 originating from a large part of southeastern Canada throughout the Quaternary (Piper et  
42 al. 2016), they host some of the largest levees in the world (Skene et al., 2002; Skene and  
43 Piper, 2003). Levees are wedge-shaped sedimentary deposits formed by deposition along  
44 the margin of channels that confine sediment density flows (Kane *et al.*, 2010). Levees  
45 consist mainly of an alternation of turbidites and hemipelagites and are often characterized  
46 by sediment waves (Migeon et al., 2001). Landslides on levees are generally localized and  
47 affect the inner levees, where the slope is steepest (e.g., Klaucke et al., 1997).

48 Canada is a signatory to the United Nations Convention on the Law of the Sea (UNCLOS);  
49 as a result, significant efforts have been made to map its extended continental shelf during  
50 the past decade. This systematic mapping has led to numerous discoveries on the seafloor,  
51 many of them related to geohazards. A large mass-transport deposit (MTD) on the Western  
52 Levee of Western Valley (WLWV), first recognized by Hughes-Clarke (1988) and Piper  
53 (1991), was recently mapped as part of Canada's extended continental shelf program. The  
54 extent of this MTD was previously unknown due to a lack of multibeam coverage and  
55 seismic stratigraphy in the region. In a region as well studied as the Laurentian Fan, such  
56 a large failure remained largely undocumented (Hughes-Clarke, 1988) and its significance  
57 in the stratigraphic record unknown.

58 In this paper, we document the slope failures on the WLWV of Laurentian Fan.  
59 Specifically, this paper addresses: 1) the geomorphology of the WLWV as a depositional  
60 and erosional environment; 2) the recurrence of submarine landslides in order to document  
61 the importance of the major WLWV MTD on external levee growth; 3) the failure style of  
62 this large MTD; and 4) its importance in the levee's stratigraphic record.

### 63 **Regional setting**

64 The Eastern Canadian continental shelf is characterized by the Laurentian Channel, a wide,  
65 deep, glacially carved cross-shelf trough (Todd, 2016). Seaward of the Laurentian Channel  
66 lies the large Quaternary Laurentian Fan (Piper, 2005). The Laurentian Fan is crossed by  
67 the Eastern and Western valleys (Fig. 1). The Eastern Valley is a 40 km-wide channel with  
68 its head starting at a depth of ~400 m; the Western Valley is narrower ( $\leq 20$  km). Both  
69 valleys are connected by a narrow Central Valley that originates from a low point on the  
70 Eastern Valley near 3000 m and joins the Western Valley near 3800 m (Fig. 1). The western  
71 levees of both the Eastern and Western Valleys are among the largest in the World (Skene  
72 et al. 2002).

73 The sedimentology and stratigraphy is well known in the study area (Mosher et al., 2004).  
74 Proglacial sedimentation is characterized by grayish brown mud with silty turbidites and  
75 ice-rafted debris overlain by red brown mud with sandy intervals and ice-rafted debris. The  
76 late Quaternary stratigraphy of the Laurentian Fan reveals that turbidite deposition ceased  
77 around 14 ka  $^{14}\text{C}$  BP (Skene and Piper, 2003). Brick red mud units linked with Heinrich  
78 events were deposited in the upper parts of this red brown mud facies and are dated to 14-  
79 13 ka  $^{14}\text{C}$  BP. Holocene sedimentation is characterized by olive gray mud and silt, often  
80 bioturbated.

81 MTDs occur on canyon walls (Jenner *et al.*, 2007), and occasionally on open slopes  
82 (Mosher *et al.*, 2004). The largest MTDs are observed deeper in the stratigraphic record,  
83 two of the largest ones being MTD-J and the 150 ka BP MTD-D (Fig. 2A). They were  
84 hypothesized to have been triggered by earthquakes and preconditioned by high glacial  
85 sedimentation (Piper & Ingram, 2003).

86 **Methods**

87 Deep-water, high-resolution bathymetric data was collected by the Geological Survey of  
88 Canada (GSC) and the Canadian Hydrographic Service (CHS) in 2012 on board the R/V  
89 Atlantis (Expedition AT22-01) using a Hull mounted 12 kHz Kongsberg EM122  
90 multibeam sonar coupled with a XYSEA PHINS integrated motion sensor. Positioning was  
91 provided by a satellite corrected CNav GPS and real-time sound speed at the transducer  
92 was acquired using a Seabird TSG velocity sounder. Expendable bathythermograph sound  
93 speed profiler casts were recalculated using the 2009 World Ocean Atlas (WOA) database  
94 salinity profiles and imported in real-time to the navigation and acquisition software (SIS).  
95 The EM122 has a 64° swath angle and 865 beams per ping. The data was imported into  
96 Caris HIPS and SIPS and gridded at a 60 m resolution. Backscatter intensity information  
97 was also recorded during the Atlantis cruise and was processed using Caris HIPS and SIPS  
98 Geocoder engine. The data were gridded at a 40 m resolution but the resolution decreases  
99 with increasing distance from nadir.

100 During the Atlantis cruise, 3.5 kHz Knudsen sub-bottom profiler data were acquired along  
101 the same lines as the multibeam data. These lines are roughly parallel to the depth contours,  
102 limiting the analysis of downslope features. In 2016, a GSC expedition on CCGS Hudson  
103 acquired seismic reflection data using a Hunttec deep-tow system with a sparker source.  
104 The acoustic output was centered on ~1.5 kHz, with a 0.5-2.5 kHz bandwidth. 3.4 L  
105 Generator-Injector (GI) gun and single channel streamer data were collected to image  
106 deeper reflections. The sub-bottom data were imported and analyzed in The Kingdom Suite  
107 software.

108 **Results**

109 *Morphology and internal architecture of the Western Levee of Western Valley*

110 The WLWV has a relief, measured as the height above the floor of Western Valley, of 650  
111 m at 3500 m water depth. Its relief progressively decreases downslope to less than 100 m  
112 at > 4700 m water depth (Fig. 1). The steep inner levee wall slope (5-6 °) consists of  
113 widespread and small scarps and gullies, even at depth of > 4500 m (Fig. 3). The eastern  
114 inner levee wall also consists of headscarps, although they are less common than on the

115 western one, where data are available. The headscarps do not appear to have a resulting  
116 deposit downslope since the latter may have been remobilized by density flows that eroded  
117 the Valley.

118 The external levee slope of WLWV has a much smoother surface compared to the inner  
119 levee slope, with a mean gradient  $\leq 1^\circ$ . This smooth appearance is due to the lower relief  
120 of the different geomorphological features observed. At a depth of  $\sim 3500$  m, the levee is  
121 composed of an aggradational spillover channel that has a 20 km-wide head narrowing  
122 downslope to 3 km (Fig. 3, 4A). The head of this channel is located near the confluence of  
123 the Western and Central Valleys, where density flows likely overspill the levee.  
124 Downslope, an unnamed channel delimits the western extent of the levee (Fig. 3).

125 The upper 0.2 s TWT of seismic profiles collected over the levee can be separated into two  
126 distinct acoustic facies. The shallower undisturbed depths consist of generally continuous,  
127 parallel medium to high-amplitude reflections (Fig. 4A) whereas the deeper areas of the  
128 levee consist of discontinuous chaotic reflections (Fig. 4B). Wavy reflections observed in  
129 the shallower parts of the levee result from the draping of underlying chaotic reflections.  
130 Near the crest of the levee, the upper reflections, i.e., those at the seafloor, often appear  
131 chaotic, reflecting small MTDs (Fig. 3A). Seismic reflections across the levee reveal that  
132 the thickness of the sediment diminishes away from the valley, consistent with higher  
133 sedimentation rates at the crest during levee growth (Fig. 2B).

#### 134 *Surficial mass transport deposit characteristics*

135 The main surficial MTD (WLWV MTD) was mapped from the bathymetry and backscatter  
136 imagery and has its shallowest headscarp at a water depth of  $\sim 4000$  m and extends down  
137 to more than 5000 m. Its basinward limit is unknown since the multibeam coverage ends  
138 at a water depth of 5000 m (Fig. 3). The MTD is more than 100 km wide and extends  
139 downslope approximately 100 km (run-out length), encompassing an area of  $> 14\,000$  km<sup>2</sup>.  
140 The headscarp of the landslide commonly reaches the crest of the levee; where it does not,  
141 it is amphitheatre shaped, arcuate to elongate in plan form, and has crown cracks along the  
142 headwalls (Fig. 5). The headscarps are 5-10 km wide and the scar slopes reach locally  $10^\circ$   
143 but are typically  $< 5^\circ$ , with heights of  $\sim 40$  m. Its run-out ratio (headscarp height vs run-out

144 length) is 0.0005, making it a long running landslide relative to its height (McAdoo et al.,  
145 2000). The adjacent undisturbed slopes are  $\leq 1^\circ$ . The proximal domain is characterized by  
146 ridges and troughs spaced 300-400 m apart gradually increasing to more than 500 m (Fig.  
147 5). The ridges and troughs morphology progressively disintegrate downslope into blocky  
148 debris and then to a smooth seafloor with lineations. In some cases, the shallower parts of  
149 the MTD have well-defined small lobe deposits that appear to overlie MTD sediments (lobe  
150 superposition; Fig. 5). The ridges and troughs lack any seismic internal structures and are  
151 chaotic. Where the headscarps reach the crest, ridges and troughs are absent and are  
152 replaced by an extensive field of blocky debris (Figs. 4B-5).

153 The backscatter response of the undisturbed sediment on the levee is relatively low and can  
154 be observed to the north (Fig. 6). The backscatter intensity increases substantially on the  
155 MTD. The multibeam bathymetry, in combination with the backscatter imagery, reveals  
156 the presence of flow lineations in a NE/SW direction. Downslope, these flow lineations  
157 abruptly stop where the MTD partly fills the unnamed channel. This channel is the  
158 westward limit of the MTD. The MTD is typically frontally confined since the unnamed  
159 channel limits frontal emergence (Fig. 4B-2A). Where the MTD does not reach this  
160 channel, frontal emergence is observed (Fig. 7A) and can easily be differentiated in the  
161 backscatter imagery (Fig. 6).

162 The 3.5 kHz acoustic stratigraphy reveals that the glide plane is a high-amplitude reflection  
163 (Figs. 4B,7). It is generally continuous from the mid levee to the toe of the MTD (Fig. 4B).  
164 Occasional erosional features, possibly grooves and erosional pits are observed (Fig. 7A).  
165 Upslope, the acoustic appearance is very chaotic, reflecting the presence of blocky debris  
166 near the crest of the levee. The thickness of the deposit is also more variable near the crest  
167 of the levee, ranging between 10 m on steeper slopes and 30 m on lower slopes. Where  
168 slopes are steeper, retrogressive headwalls are observed (Fig. 7B).

## 169 **Discussion**

### 170 *Landslide behaviour*

171 The landslide can be divided into three zones of different failure types (Figs 4, 5): 1) Zone  
172 1 is characterized by extensional spreading of the seabed; 2) Zone 2 is characterized by an

173 extensive blocky debris field and; 3) Zone 3 consists of disintegrated blocks and likely  
174 represents a complex slide with a debris flow overlying a blocky landslide.

175 The ridge and trough morphology is characteristic of spreads, a type of failure  
176 characterized by the failure of sediment into coherent blocks displaced downslope along a  
177 glide plane (e.g., Micallef et al., 2007; Baeten et al., 2013). The spreading component of  
178 the MTD is confined to the amphitheater shaped scarps that did not reach the crest of the  
179 levee. These cohesive blocks were displaced downslope along a planar gliding plane.  
180 Spreading is also often indicative of headscarp retrogression, which is further observed by  
181 the presence of multiple headwalls in the sub-bottom profiles (Fig. 7B). The spreading  
182 retrogressed upslope and disintegrated downslope into a blocky debris MTD and finally  
183 into a debris flow. The spreading component of the MTD is absent in some places because  
184 the retrogression reached the crest of the levee and was completely evacuated as a blocky  
185 landslide (Fig. 4B). Retrogression to the levee crest may indicate little change in upslope  
186 sediment strength that would have been able to stop the retrogression. The possible  
187 grooves, or at least local erosion of the glide plane (Fig. 7A), indicate that large intact  
188 blocks within the blocky MTD eroded the seabed during downslope movement or that the  
189 glide plane was not confined to a single stratigraphic level. Such intact blocks are not  
190 observed on the sub-bottom data, perhaps because of the large acoustic footprint making it  
191 impossible to resolve such features or because they disintegrated following the localized  
192 erosion of the glide plane. The debris flow extends down the flank of the external levee,  
193 eventually terminating in an unnamed channel that runs parallel to Western Valley (Fig.  
194 2). To the south, away from this unnamed channel, the MTD displays frontally emergent  
195 characteristics, that is, the deposit ramps up from its original basal shear surface (Frey-  
196 Martinez *et al.*, 2006) (Fig. 6-7A).

197 The upslope spreading zone likely formed in two ways: 1) it could have resulted from the  
198 initial development of the large landslide during one main event with rapid retrogression  
199 of the headscarp; or 2) it could have formed following an initial phase of mass transport  
200 during multiple and distinct events. The sliding of material downslope can cause a loss of  
201 support for the upslope sediment, which can be reactivated during a later, distinct trigger  
202 event. There is also evidence from lobe superimposition that evacuation of the main MTD

203 led to a loss of support in the upslope part of the levees, which could have caused upslope  
204 spreading (Fig. 5).

205 In any case, the blocky debris flow is likely the result of disintegration of an initial spread.  
206 The blocks at the distal edge of the spread were displaced downslope and disintegrated  
207 when passing over the pre-existing headwalls (e.g., Piper et al., 1999; Micallef et al., 2007).  
208 This process is illustrated in Fig. 7B where a blocky debris field thins over a steeper slope  
209 with buried retrogressive headwalls and thickens as a homogeneous acoustic unit  
210 downslope. The 3.5 kHz consistently reveals incoherent acoustic reflections within the  
211 deposit, suggesting disintegration of the failed deposit and its homogenization during  
212 transport. These surficial sediments broke up easily during transport because of the  
213 presence of thin sand and silt turbidites that shear during downslope movement (Piper et  
214 al., 2012).

#### 215 *Timing of submarine landslides*

216 Landslides on the internal slope of the WLWV are suspected to have occurred frequently  
217 during the Pleistocene according to the number of landslide scarps visible on the multibeam  
218 imagery. The presence of these landslides is also consistent with the frequent passage of  
219 sediment density flows in the channel during the glacial period (Skene and Piper, 2003)  
220 which caused erosion, undercutting and oversteepening of the channel wall. However,  
221 landslides are comparatively infrequent on the lower gradients ( $<1^\circ$ ) of the external levee.  
222 Small landslides are present near the crest of the levee but long-running ones reaching the  
223 base of slope are infrequent (Fig. 2B). The most recent MTD appears to be the largest on  
224 the levee.

225 Piper (1991) initially suggested that the largest landslide on the WLWV was triggered  
226 during the Holocene solely based on its presence in the upper stratigraphic succession. The  
227 high-resolution imagery presented here provides additional support for a late-Pleistocene /  
228 Holocene age of the MTD. The debris flow component of the MTD extends ~ 90 km  
229 downslope and partially fills an unnamed submarine channel. The filling of the channel  
230 and the location of the MTD at the top of the stratigraphic succession on the levee suggests  
231 that it occurred after major canyon flow events ceased and is possibly post-glacial in age.



232 The major gravity flows in submarine canyons along the Scotian margin have been active  
233 until *ca* 14 ka <sup>14</sup>C BP (Skene and Piper, 2003), which suggests that turbidity currents would  
234 have eroded/alterd the MTD if it had been triggered prior to deglaciation.

235 Although the main event most likely occurred during the late-Pleistocene / Holocene,  
236 smaller components of the landslide may have occurred more recently. Evidence of smaller  
237 landslide activity following the main event is observed near the crest of the levee. For  
238 example, a deposit appears to overlie the main blocky MTD (Fig. 5). Additionally, the  
239 presence of crown cracks suggests that the landslide may not be in a stable state. Crown  
240 cracks typically indicate incipient failure that could be ongoing in the region (e.g., Micallef  
241 et al., 2007; Li et al., 2016). Therefore, although the main landslide may have been  
242 triggered during the late Pleistocene or early Holocene, it could have been reactivated  
243 locally after the initial failure.

#### 244 *Significance in the stratigraphic record and geohazard implications*

245 A large MTD on the WLWV was first identified by Hughes-Clarke (1988) and Piper  
246 (1991) based on sparse echosounder profiles. At the time, its submarine extent,  
247 geomorphology and importance in the stratigraphic record was unclear due to lack of data.  
248 The newly acquired multibeam bathymetric data allows us to identify it as one of the largest  
249 MTDs observed in the Western North Atlantic with an area of > 14 000 km<sup>2</sup>. According to  
250 Lee et al. (2007), only 2% of the landslides on the United States margin have an area larger  
251 than 1000 km<sup>2</sup> and the largest is estimated at 19 000 km<sup>2</sup>. On the Canadian margin, it is the  
252 largest surficial landslide identified to date although larger landslides were identified in the  
253 stratigraphic record, namely the ~93 000 km<sup>2</sup> Montagnais landslide (Deptuck and  
254 Campbell, 2012). In the North Atlantic, this landslide is also among the deepest at 4000 m  
255 (Huhnerbach and Masson, 2004). Most landslides on the Scotian margin were initiated on  
256 the upper slope and evolved on the lower slope. The WLWV landslide initiated on the  
257 lower Scotian Slope and still led to one of the largest MTD in the region. Its presence in  
258 deep-water and on low angle slopes, its size and its young age make it a significant event  
259 to have occurred in the North Atlantic.

260 Small MTDs are recognized on the external levee of WLWV but are generally restricted  
261 to its upper parts. On the other hand, extensive MTDs disturbing the entire external levee  
262 appear to be extremely rare in the stratigraphic record. Deep seismic reflection data show  
263 that during the Quaternary, the shallowest MTD is also the largest one observed in the  
264 upper ~375 m of the levee succession. In the stratigraphic record of the Nova Scotia  
265 continental slope, the WLWV MTD is among the largest reported. Piper and Ingram (2003)  
266 described a series of Quaternary sediment failures on the east lower Scotian Slope, the  
267 largest, MTD-D (Fig. 4B), estimated to have occurred at ~150 ka BP. These MTDs were  
268 described as originating from the continental slope. The known extent of MTD-D is ~ 8  
269 000 km<sup>2</sup>. However, the new seismic profiles show that the areal extent of MTD-D may be  
270 two times greater. Therefore, in terms of areal extent, MTD-D and the WLWV MTD are  
271 similar. The volumes of failure are likely different since Fig. 2A clearly shows that MTD-  
272 D is much thicker than WLWV MTD. The volume of sediment involved in MTD-D is  
273 estimated at 800 km<sup>3</sup> whereas the volume of sediment involved in WLWV MTD is  
274 estimated at 300-400 km<sup>3</sup>. Nonetheless, the WLWV MTD is the largest late-Pleistocene /  
275 Holocene MTD on the Scotian margin identified to date, making it much younger than the  
276 ones described by Piper and Ingram (2003). It also remobilized a much larger volume than  
277 the 1929 earthquake-induced turbidite, the latter involving 150 km<sup>3</sup> of failed material  
278 (Piper and Aksu, 1987). This giant landslide is thus a significant event in the late  
279 Quaternary record of the Scotian Slope.

280 Most landslides on the Scotian margin are believed to have been triggered by earthquakes  
281 (Piper and McCall, 2003). In this particular case, the earthquake trigger appears likely since  
282 two coeval MTDs are observed on the levee (Fig. 3). Unique geological setting may also  
283 be partly responsible for this event since it is located on one of the largest levees in the  
284 world, an emplacement that differs from other large MTDs. External levees are typically  
285 characterized by sediment waves with little evidence of MTDs (e.g., Migeon et al., 2001),  
286 which are generally observed on the inner levee walls. However, it is worth noting that the  
287 large accumulation of sediments on the levee as well as the alternation of hemipelagites  
288 and turbidites favour the presence of weak layers (Cauchon-Voyer et al. 2008) which in  
289 turn favour the occurrence of landslides. In this respect, levee MTDs are similar to

290 contourite drifts where failures may be due to low shear strength owing to high  
291 sedimentation rates and well sorted sediment, underconsolidation, and loading due to  
292 earthquakes and overlying sediment (Laberg and Camerlenghi, 2008). Although  
293 earthquakes are rare in the region, they do occur preferentially along the Laurentian Fan  
294 region, most notably being the M7.2 1929 event (Mazzotti, 2007). Other earthquakes may  
295 have occurred during the Holocene (e.g., Piper et al., 1985) but are insufficiently  
296 documented at present.

### 297 **Conclusion**

298 Recently-acquired multibeam bathymetry data expose the presence of one of the most  
299 extensive MTDs in the Western North Atlantic, covering an area of > 14 000 km<sup>2</sup>. The  
300 results from this study reveal that:

- 301 1) The landslide initiated as a retrogressive spread that rapidly evolved downslope as  
302 a blocky debris landslide. The retrogression reached the crest of the levee in a large  
303 part of the region, leading to its disintegration as a debris flow;
- 304 2) The MTD filled an unnamed channel downslope and is located at the top of the  
305 stratigraphic succession, suggesting it is late-Pleistocene to Holocene in age,  
306 making it one of the most recent major landslides on the Scotian Slope;
- 307 3) The presence of multiple headwalls and lobe superimposition suggest that the  
308 landslide evolved in a multi-stage fashion. The crown cracks near the headscarp  
309 also suggest that the landslide may not be in stable state and that instability may  
310 still be ongoing;
- 311 4) This landslide event is a rare deep-water event. It is also a rare event to have  
312 occurred on the WLWV, a levee dominated by turbidite/hemipelagite deposition.

313 This giant MTD is thus the record of a major event in the late-Quaternary of the Scotian  
314 Slope and its significance was only just discovered as part of Canada's extended  
315 continental shelf program under UNCLOS. Such systematic mapping programs are thus  
316 vital for the evaluation of geohazards on continental margins. Further investigations of this

317 MTD should be accomplished in order to determine how it evolved during the Holocene  
318 and to evaluate whether or not it is in a stable state.

319 **Acknowledgements**

320 The authors thank the Atlantis AT22-1 and Hudson 2016-011 Phase 1 participants for their  
321 help during data acquisition. Support for this project was from the Geological Survey of  
322 Canada.

323 **References**

- 324 BAETEN, N.J., LABERG, J.S., ET AL. 2013. Morphology and origin of smaller-scale mass  
325 movements on the continental slope off northern Norway. *Geomorphology*, **187**,  
326 122–134, doi: 10.1016/j.geomorph.2013.01.008.
- 327 CAUCHON-VOYER, G., LOCAT, J. & ST-ONGE, G. 2008. Late-Quaternary morpho-  
328 sedimentology and submarine mass movements of the Betsiamites area, Lower St.  
329 Lawrence Estuary, Quebec, Canada. *Marine Geology*, **251**, 233–252, doi:  
330 10.1016/j.margeo.2008.03.003.
- 331 DEPTUCK, M. & CAMPBELL, D.C. 2012. Widespread erosion and mass failure from the 51  
332 Ma Montagnais marine bolide impact off southwestern Nova Scotia, Canada.  
333 *Canadian Journal of Earth Sciences*, **49**, 1567–1594, doi: 10.1139/e2012-070.
- 334 FREY-MARTINEZ, J., CARTWRIGHT, J. & JAMES, D. 2006. Frontally confined versus  
335 frontally emergent submarine landslides: A 3D seismic characterisation. *Marine and*  
336 *Petroleum Geology*, **23**, 585–604, doi: 10.1016/j.marpetgeo.2006.04.002.
- 337 HAMPTON, M.A., LEE, H.J. & LOCAT, J. 1996. Submarine landslides. *Reviews of*  
338 *Geophysics*, **34**, 33–59, doi: 10.1029/95rg03287.
- 339 HUGHES-CLARKE, J.E. 1988. *The Geological Record of the 1929 Grand Banks''*  
340 *Earthquake and Its Relevance to Deep-Sea Clastic Sedimentation*. Dalhousie  
341 University.
- 342 HUHNERBACH, V. & MASSON, D.G. 2004. Landslides in the North Atlantic and its  
343 adjacent seas : an analysis of their morphology , setting and behaviour. *Marine*

- 344 *Geology*, **213**, 343–362, doi: 10.1016/j.margeo.2004.10.013.
- 345 JENNER, K.A., PIPER, D.J.W., CAMPBELL, D.C. & MOSHER, D.C. 2007. Lithofacies and  
346 origin of late Quaternary mass transport deposits in submarine canyons, central  
347 Scotian Slope, Canada. *Sedimentology*, **54**, 19–38, doi: 10.1111/j.1365-  
348 3091.2006.00819.x.
- 349 KANE, I.A., McCAFFREY, W.D., PEAKALL, J. & KNELLER, B.C. 2010. Submarine channel  
350 levee shape and sediment waves from physical experiments. *Sedimentary Geology*,  
351 **223**, 75–85, doi: 10.1016/j.sedgeo.2009.11.001.
- 352 KLAUCKE, I., HESSE, R. & RYAN, W.B.F. 1997. Flow parameters of turbidity currents in a  
353 low-sinuosity giant deep-sea channel. *Sedimentology*, **44**, 1093–1102, doi:  
354 10.1111/j.1365-3091.1997.tb02180.x.
- 355 LABERG, J.S. & CAMERLENGHI, A. 2008. The Significance of Contourites for Submarine  
356 Slope Stability. In: Rebesco, M. & Camerlenghi, A. (eds) *Contourites*. Elsevier,  
357 537–556., doi: 10.1016/S0070-4571(08)10025-5.
- 358 LEE, H., LOCAT, J., ET AL. 2007. Submarine mass movements on continental margins. In:  
359 Nittrouer, C. A., Austin Jr, J. A., Field, M., Kravitz, J. H., Syvitski, J. P. M. &  
360 Wiberg, P. L. (eds) *Continental Margin Sedimentation: From Sediment Transport to*  
361 *Sequence Stratigraphy*. Malden, MA, Wiley, Book Section, 213–274., doi:  
362 10.1002/9781444304398.
- 363 LEE, H.J. 2009. Timing of occurrence of large submarine landslides on the Atlantic  
364 Ocean margin. *Marine Geology*, **264**, 53–64, doi: 10.1016/j.margeo.2008.09.009.
- 365 LI, W., ALVES, T.M., ET AL. 2016. Morphology, age and sediment dynamics of the upper  
366 headwall of the Sahara Slide Complex, Northwest Africa: Evidence for a large Late  
367 Holocene failure. *Marine Geology*, doi:  
368 <http://dx.doi.org/10.1016/j.margeo.2016.11.013>.
- 369 MAZZOTTI, S. 2007. Geodynamic models for earthquake studies in intraplate North  
370 America. *The Geological Society of America, Special Paper*, **425**, 17–33, doi:  
371 10.1130/2007.2425(02).

- 372 MCADOO, B.G., PRATSON, L.F. & ORANGE, D.L. 2000. Submarine landslide  
373 geomorphology, US continental slope. *Marine Geology*, **169**, 103–136.
- 374 MICALLEF, A., MASSON, D.G., BERNDT, C. & STOW, D.A. V. 2007. Morphology and  
375 mechanics of submarine spreading: A case study from the Storegga Slide. *Journal of*  
376 *Geophysical Research: Earth Surface*, **112**, 1–21, doi: 10.1029/2006JF000739.
- 377 MIGEON, S., SAVOYE, B., ZANELLA, E., MULDER, T., FAUGERES, J.-C. & WEBER, O.  
378 2001a. Detailed seismic-reflection and sedimentary study of turbidite sedimentwaves  
379 on the Var Sedimentary Ridge (SE France): significance for sediment transport and  
380 deposition and for the mechanisms of sediment-wave construction. *Marine And*  
381 *Petroleum Geology*, **18**, 179–208.
- 382 MIGEON, S., SAVOYE, B., ZANELLA, E., MULDER, T., FAUGÈRES, J.C. & WEBER, O.  
383 2001b. Detailed seismic-reflection and sedimentary study of turbidite sediment  
384 waves on the Var Sedimentary Ridge (SE France): significance for sediment  
385 transport and deposition and for the mechanisms of sediment-wave construction.  
386 *Marine and Petroleum Geology*, **18**, 179–206.
- 387 MOSHER, D.C., PIPER, D.J.W., CALVIN CAMPBELL, D. & JENNER, K.A. 2004. Near-  
388 surface geology and sediment-failure geohazards of the central Scotian Slope. *AAPG*  
389 *Bulletin*, **88**, 703–723, doi: 10.1306/01260403084.
- 390 PIPER, D.J.W. 1991. Surficial geology and physical properties 6: deep water surficial  
391 geology. *In: Scotian Shelf*. 121., doi: 10.4095/210698.
- 392 PIPER, D.J.W. 2005. Late Cenozoic evolution of the continental margin of eastern  
393 Canada. *Norwegian Journal of Geology*, **85**, 305–318.
- 394 PIPER, D.J.W. & AKSU, A.E. 1987. The source and origin of the 1929 grand banks  
395 turbidity current inferred from sediment budgets. *Geo-Marine Letters*, **7**, 177–182.
- 396 PIPER, D.J.W. & INGRAM, S. 2003. Geological Survey of Canada Major Quaternary  
397 sediment failures on the east Scotian Rise, eastern Canada. *Current Research -*  
398 *Geological Survey of Canada*, 1–7.
- 399 PIPER, D.J.W. & MCCALL, C. 2003. A Synthesis of the Distribution of Submarine Mass

- 400 Movements on the Eastern Canadian Margin. *In*: Locat, J. & Mienert, J. (eds)  
401 *Submarine Mass Movements and Their Consequences*. Springer Netherlands, 291–  
402 298., doi: 10.1007/978-94-010-0093-2.
- 403 PIPER, D.J.W., FARRE, J.A. & SHOR, A. 1985. Late Quaternary slumps and debris flows  
404 on the Scotian Slope. *Geological Society of America Bulletin*, **96**, 1508–1517.
- 405 PIPER, D.J.W., COCHONAT, P. & MORRISON, M.L. 1999. The sequence of events around  
406 the epicentre of the 1929 Grand Banks earthquake: initiation of debris flows and  
407 turbidity current inferred from sidescan sonar. *Sedimentology*, **46**, 79–97.
- 408 PIPER, D.J.W., MOSHER, D.C., GAULEY, B.J., JENNER, K. & CAMPBELL, D.C. 2003. The  
409 chronology and recurrence of submarine mass movements on the continental slope  
410 off southeastern Canada. *In*: Locat, J. & Mienert, J. (eds) *Submarine Mass*  
411 *Movements and Their Consequences, Advances in Natural and Technological*  
412 *Hazards Research*. Springer Netherlands, 299–306.
- 413 PIPER, D.J.W., MOSHER, D.C. & CAMPBELL, D.C. 2012. Controls on the distribution of  
414 major types of submarine landslides. *In*: Clague, J. J. & Stead, D. (eds) *Landslides:*  
415 *Types, Mechanisms and Modeling*. Cambridge University Press, 95–107.
- 416 PIPER, D.J.W., CAMPBELL, D.C. & MOSHER, D.C. 2016. Mid-latitude complex trough-  
417 mouth fans, Laurentian and Northeast fans, eastern Canada. *In*: Dowdeswell, J. A.,  
418 Canals, M., Jakobsson, M., Todd, B. J., Dowdeswell, E. . & Hogan, K. A. (eds)  
419 *Atlas of Submarine Glacial Landforms: Modern, Quaternary and Ancient*. London,  
420 Geological Society, 363–364., doi: 10.1144/M46.93.
- 421 SKENE, K.I. & PIPER, D.J.W. 2003. Late Quaternary stratigraphy of Laurentian Fan: A  
422 record of events off the eastern Canadian continental margin during the last  
423 deglacial period. *Quaternary International*, **99–100**, 135–152, doi: 10.1016/S1040-  
424 6182(02)00116-7.
- 425 SKENE, K.I., PIPER, D.J.W. & HILL, P.R. 2002. Quantitative analysis of variations in  
426 depositional sequence thickness from submarine channel levees. *Sedimentology*, **49**,  
427 1411–1430.

- 428 SMITH, D.P., RUIZ, G., KVITEK, R. & IAMPIETRO, P.J. 2005. Semiannual patterns of  
429 erosion and deposition in upper Monterey Canyon from serial multibeam  
430 bathymetry. *Geological Society of America Bulletin*, **117**, 1123–1133, doi:  
431 10.1130/b25510.1.
- 432 TODD, B.J. 2016. The Laurentian Channel : a major cross-shelf trough in Atlantic  
433 Canada. *In*: Dowdeswell, J. A., Canals, M., Jakobsson, M., Todd, B. J., Dowdeswell,  
434 E. . & Hogan, K. A. (eds) *Atlas of Submarine Glacial Landforms: Modern,*  
435 *Quaternary and Ancient*. London, Geological Society, 161–162.
- 436
- 437



438 **Figures**

439 **Figure 1:** Location of Laurentian Fan and the Western Levee of Western Valley (black  
440 frame) off of the eastern Canadian continental margin. EV: Eastern Valley, CV: Central  
441 Valley, WV: Western Valley

442 **Figure 2:** GI-gun seismic profiles illustrating A) the surficial MTD in relation to the  
443 unnamed channel and a large 150 ka MTD (MTD-D); B) the stratified levee deposits and  
444 the occurrence of mass-transport deposits (MTD). Red polygons represent buried MTDs.

445 **Figure 3:** Multibeam bathymetry (60 m grid) of the Western Levee of Western Valley  
446 illustrating the spillover channel and the large mass-transport deposit (WLWV MTD).

447 **Figure 4:** Sub-bottom profiles (3.5 kHz) of the two main acoustic facies observed in the  
448 upper stratigraphic succession of the levee: A) high-amplitude reflections with occasional  
449 small mass-transport deposits (MTD) and B) chaotic to incoherent acoustic facies  
450 representing the major WLWV MTD affecting a large part of the levee.

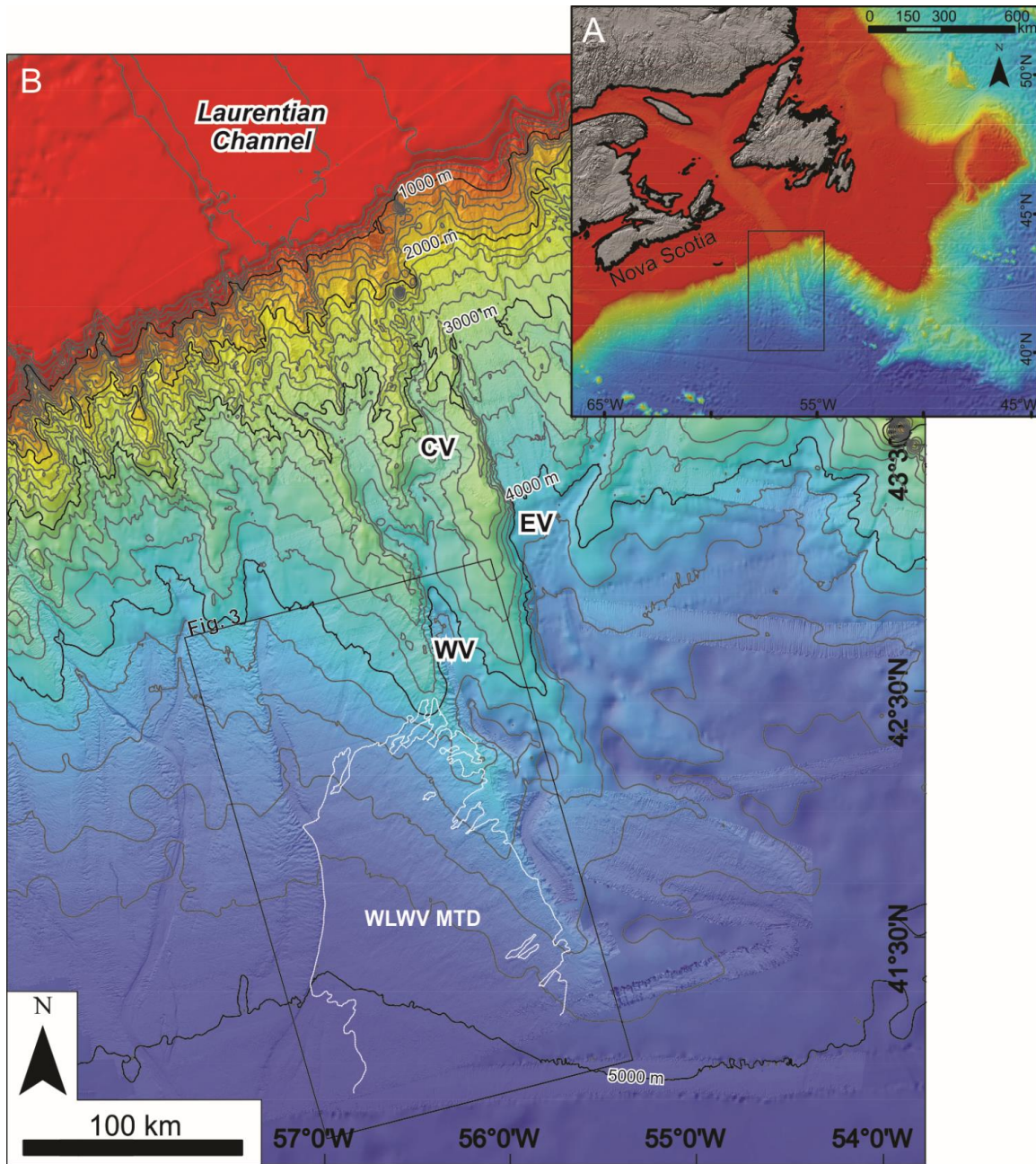
451 **Figure 5:** Multibeam bathymetry of the upper levee illustrating the different  
452 geomorphological features present, including ridges and troughs, blocky debris zone,  
453 crown cracks and lobe superposition.

454 **Figure 6:** Backscatter map of the Western Levee of Western Valley illustrating the higher  
455 intensity over the mass-transport deposit and flow lineations.

456 **Figure 7:** Hunttec and sub-bottom profiles (3.5 kHz) of the Western levee illustrating A)  
457 erosion of the glide plane and emergence at the toe of the MTD and B) retrogressive  
458 headwalls in the upper parts of the levee. Red polygon represents a buried MTD.

459

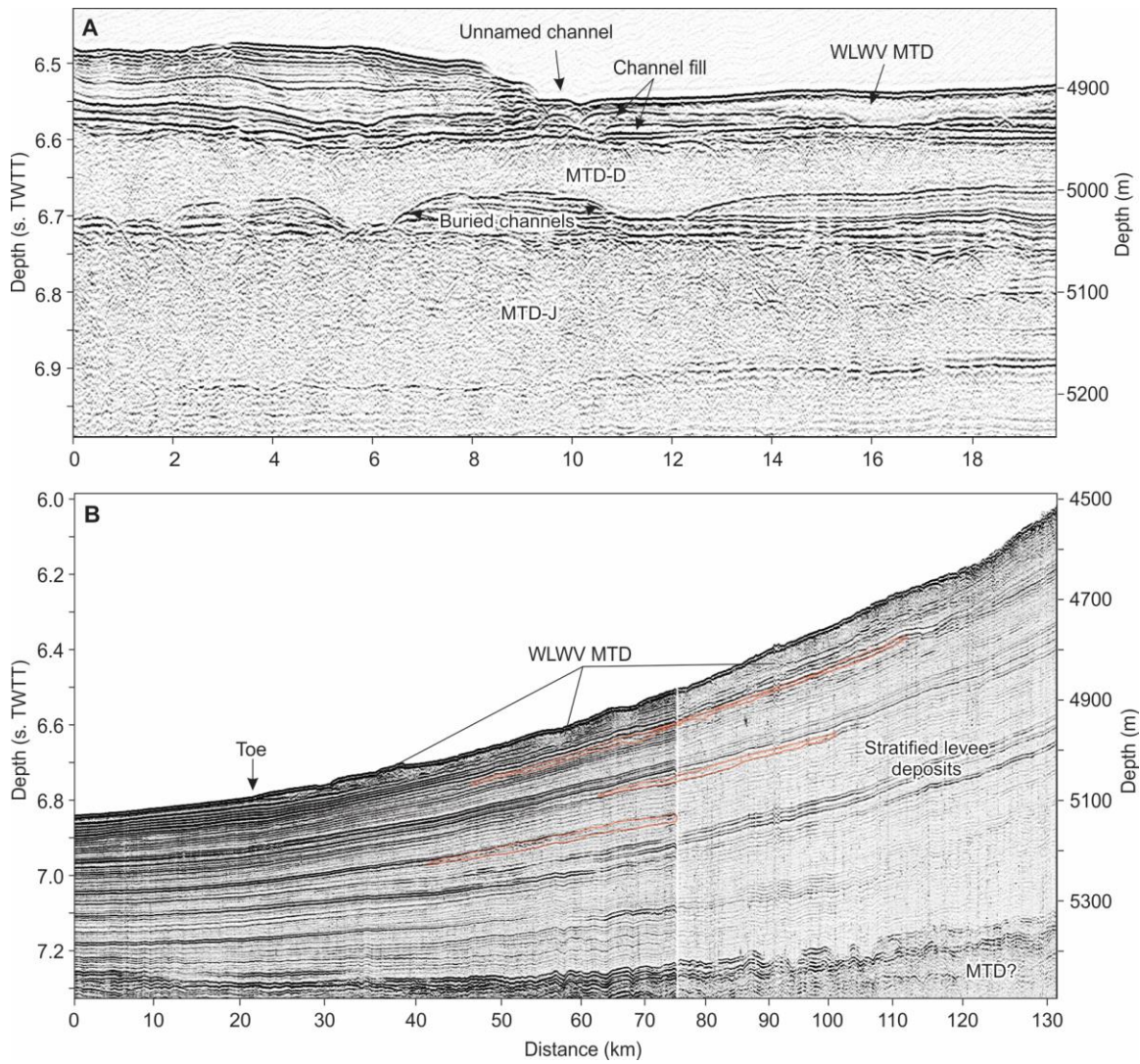
460 Figure 1



461

462

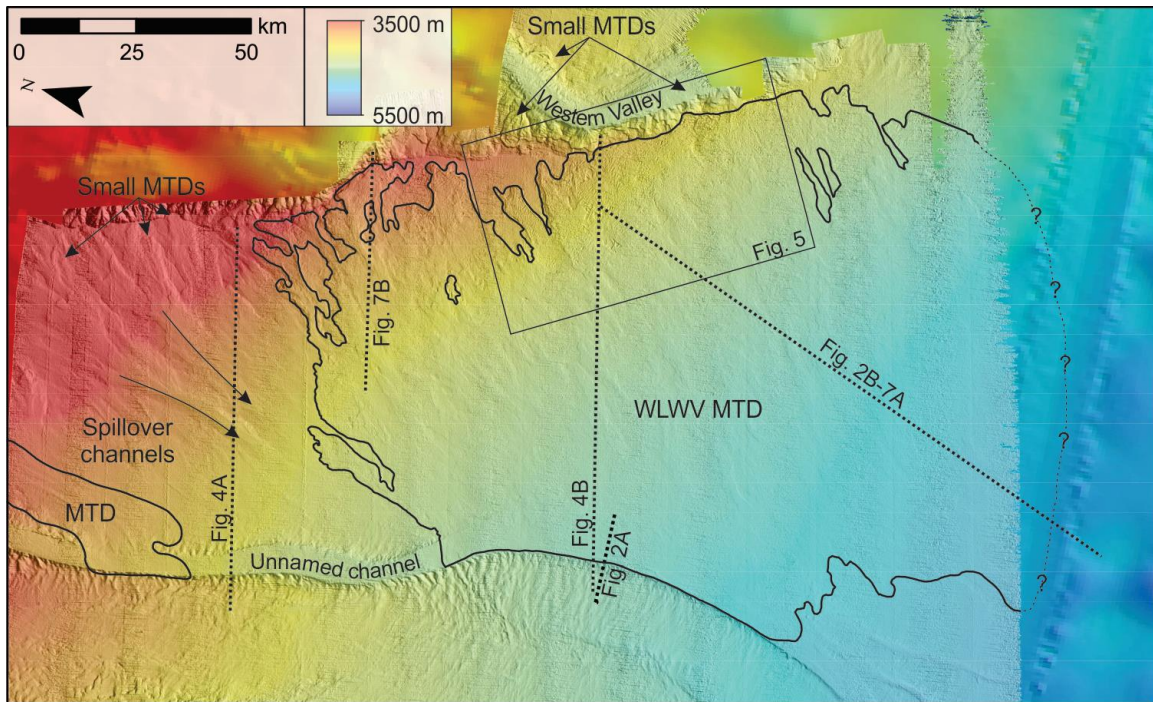
463 Figure 2



464

465

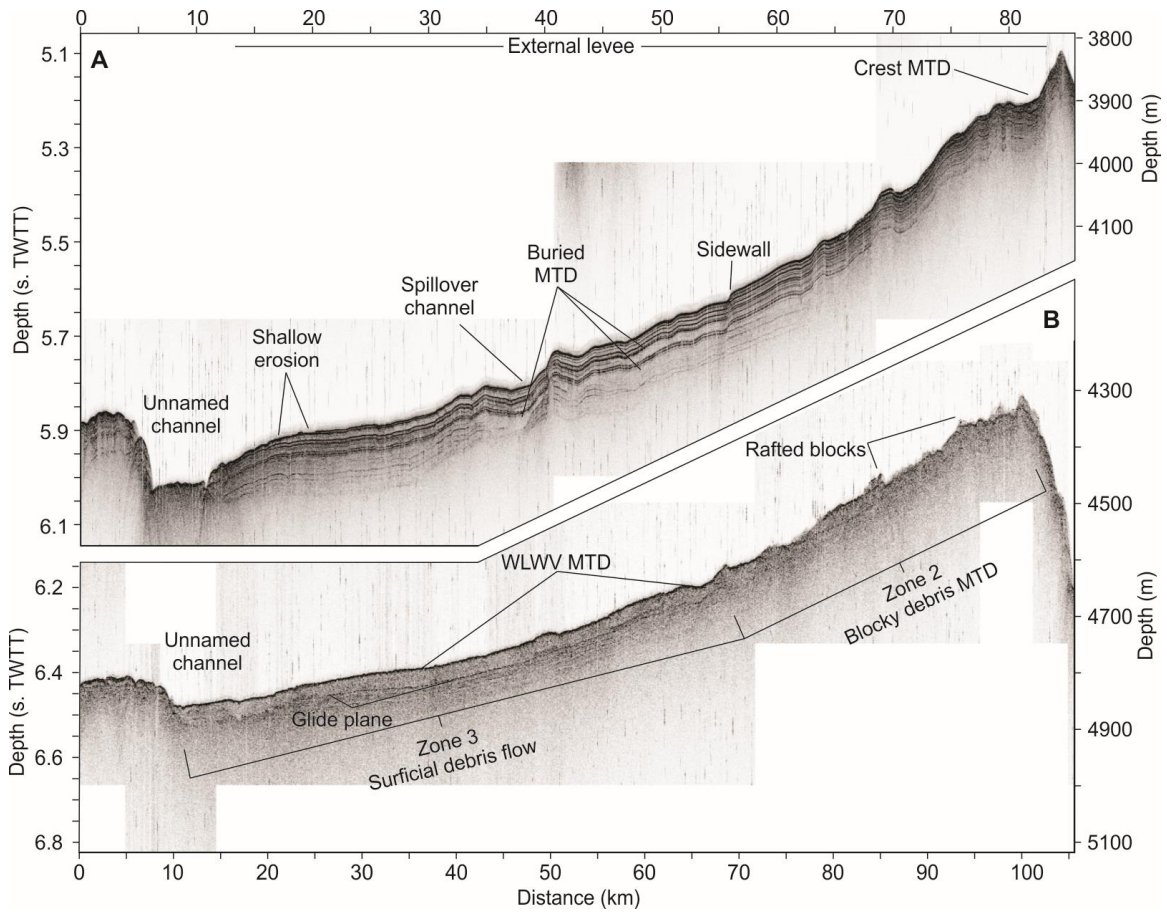
466 Figure 3



467

468

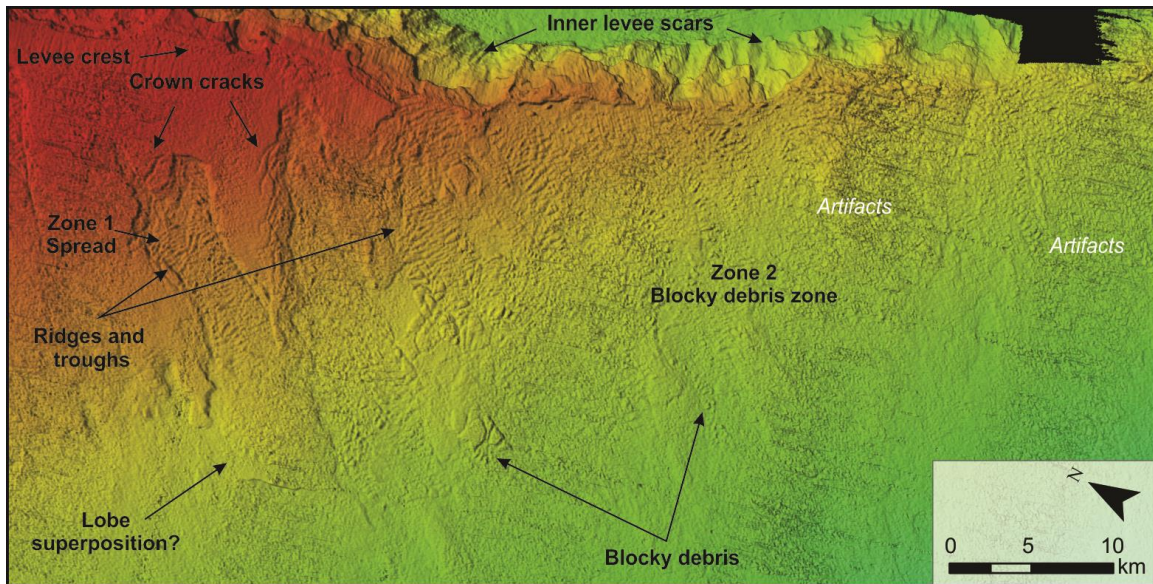
469 Figure 4



470

471

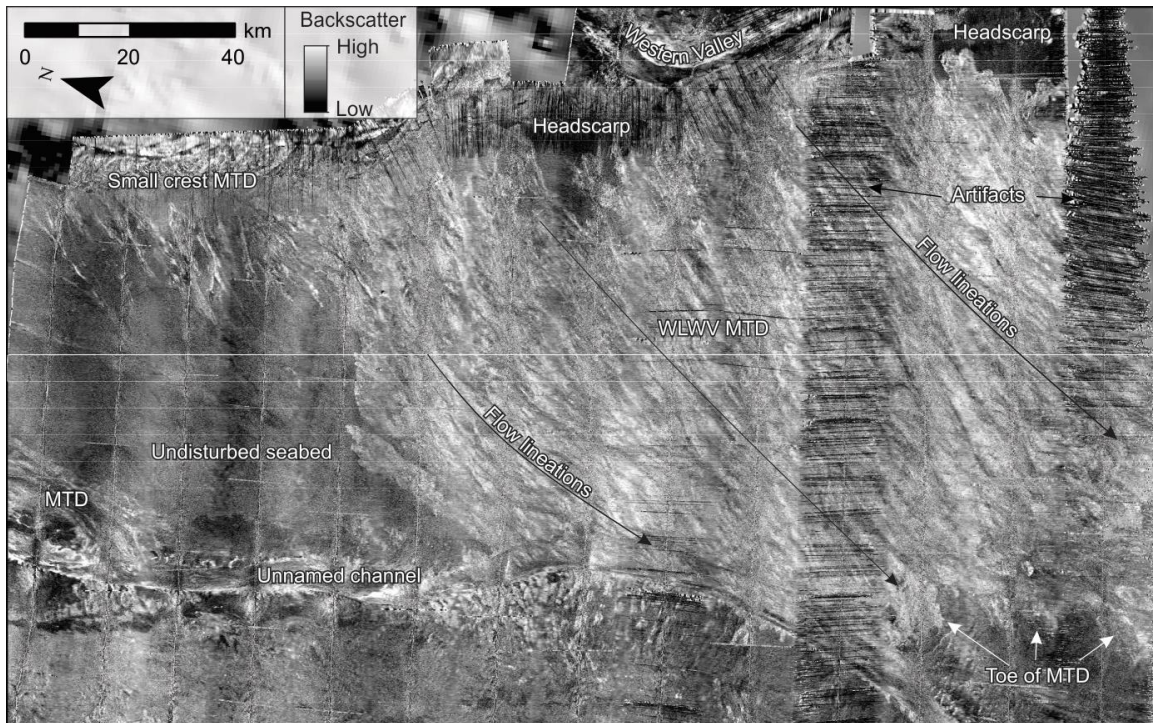
472 Figure 5



473

474

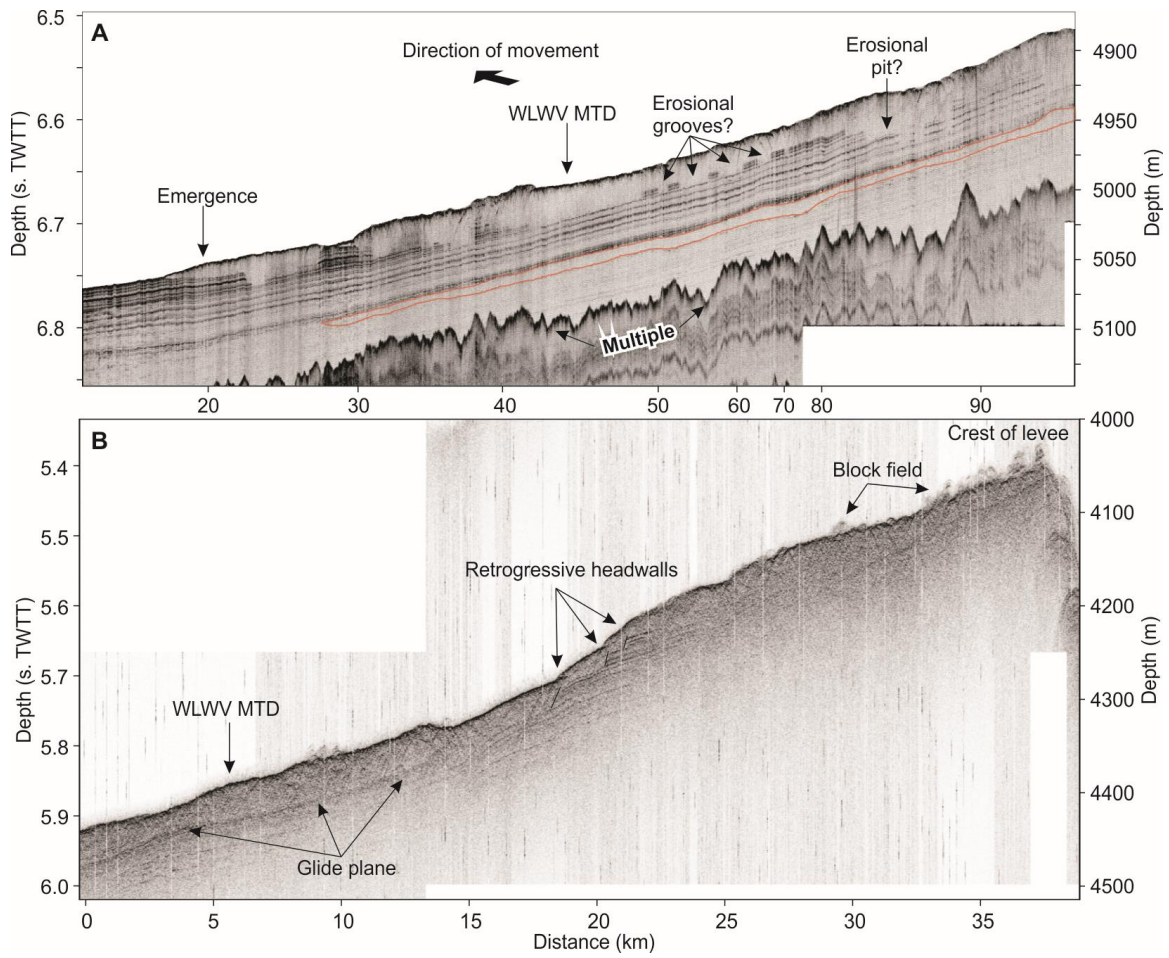
475 Figure 6



476

477

478 Figure 7



479